Journal of Cellular Biochemistry 89:133–143 (2003)

AIDS-Related Kaposi's Sarcoma Cells Rapidly Internalize Endostatin, Which Co-Localizes to Tropomysin Microfilaments and Inhibits Cytokine-Mediated Migration and Invasion

Susan R. Mallery,[1,3]* Mark A. Morse,[2,3] Ralph F. Wilson,[1] Ping Pei,[1] Gregory M. Ness,[1] Jennifer E. Bradburn,[1] Robert J. Renner,[1] David E. Schuller,[2,4] and Fredika M. Robertson[3,5]

[1]Departments of Oral Maxillofacial Surgery and Pathology and Periodontology, College of Dentistry, Ohio State University, Columbus, Ohio
[2]Division of Environmental Health Sciences, School of Public Health, College of Medicine, Ohio State University, Columbus, Ohio
[3]The Ohio State University Comprehensive Cancer Center, Ohio State University, Columbus, OH
[4]James Cancer Hospital and Solove Research Institute, Ohio State University, Columbus, OH
[5]Department of Molecular Virology, Immunology, and Medical Genetics, College of Medicine, Ohio State University, Columbus, Ohio

Abstract AIDS-related Kaposi's sarcoma (KS) is the most common HIV-related malignancy. In some respects, KS is analogous to other angioproliferative diseases, in that KS lesions are highly vascularized and promoted by inflammatory cytokines. However, unlike other cancers or inflammatory mediated vascular diseases, KS is unique in that the KS lesional cells both express and respond to the complete angiogenic cytokines vascular endothelial growth factor (VEGF) and basic fibroblast growth factor (bFGF). Therefore, the angiogenic phenotype, which is crucial for cancer progression, is inherent to KS tumor cells. Due to the recognized importance of angiogenesis in cancer progression, numerous angiostatic agents are being investigated as potential therapeutic agents. One such agent is endostatin, which is a 20-kDa carboxyl-terminal fragment of collagen XVIII that has demonstrated potent angiostatic activities at both the in vivo and in vitro levels. Since endostatin is recognized as a potent angiostatic agent, the majority of in vitro endostatin studies have evaluated its effects on endothelial cells. Although KS cells are speculated to arise from endothelial cell precursors and KS lesions are highly vascularized, no previous studies have investigated endostatin–KS cell interactions. This present study evaluated endostatin's effects on KS tumor cell: (i) signal transduction (endostatin internalization and transcription factor activation), and (ii) migration and invasion (functional activity assays and tropomysin co-localization). Our results show that KS cells rapidly internalize endostatin and that endostatin initiates activation of the transcription activating factors nuclear factor-κB (NF-κB) and activating protein 1 (AP-1). Our data also show that internalized endostatin co-localizes to tropomysin microfilaments and acts to inhibit KS cell migration and invasion in response to the clinically relevant angiogenic cytokines VEGF and bFGF. As a consequence of its combined angiostatic and antitumorigenic activities, endostatin could provide dual therapeutic benefits for patients with mucocutaneous KS. J. Cell. Biochem. 89: 133–143, 2003.

Key words: angiostatic agents; Kaposi's sarcoma; angiogenesis; migration; invasion; tumorigenesis

Ralph F. Wilson is the recipient of the Ohio Division of the American Cancer Society Research Fellowship.

David E. Schuller is the Director of James Cancer Hospital and Solove Research Institute.

Grant sponsor: NIH/NIDCR; Grant numbers: PO1 DE 12704, UO1 CA 66531, and P30 CA 16058.

*Correspondence to: Dr. Susan R. Mallery, Department of Oral Maxillofacial Surgery and Pathology, 305 W 12th Ave., P.O. Box 182357, Columbus, Ohio 43218-2357.
E-mail: mallery.1@osu.edu

Received 3 January 2003; Accepted 6 January 2003
DOI 10.1002/jcb.10489

Both clinical and experimental evidence imply that AIDS-related Kaposi's sarcoma (KS) is initially an angioproliferative hyper plasia that employs autocrine and paracrine growth loops to facilitate progression to a highly angiogenic sarcoma [Miles, 1994; Jacobson and Arnemian, 1995]. Analogous to other angioproliferative diseases such as rheumatoid arthritis, KS lesions are highly vascularized and promoted by inflammatory cytokines. However, in contrast to other cancers or inflammatory mediated diseases, KS is unique in that the KS lesional spindle cells both express and respond to the potent and complete angiogenic cytokines basic fibroblast growth factor (bFGF) and vascular endothelial growth factor (VEGF) [Miles et al., 1990; Masood et al., 1997; Samaniego et al., 1998]. Consequently, neovascularization is intimately associated with KS progression. During angiogenesis, endothelial cells invade and infiltrate surrounding tissues, where they undergo division and differentiation into microtubules [Folkman and Shing, 1992]. Similar to their putative endothelial origin progenitor cells [Rutger et al., 1986], KS cells possess migratory and invasive properties that facilitate KS angiogenesis and tumorigenesis.

Due to the recognized importance of angiogenesis in cancer progression, numerous angiostatic agents are currently being investigated as potential therapeutic agents [Folkman, 1995; Gasparini, 1999]. One such agent is endostatin, which is a 20-kDa carboxyl-terminal fragment of collagen XVIII discovered by O'Reilly et al. [1997]. Although the mechanism(s) of action of endostatin has not been completely delineated, several studies have provided mechanistic insights. While immobilized endostatin serves as an integrin agonist that facilitates cell migration, soluble endostatin perturbs integrin–substrate interactions, and inhibits cell attachment and migration [Rehn et al., 2001]. Studies that investigated endostatin's effects on intracellular signaling showed soluble endostatin initiated pathways that reduced expression of a bank of growth-associated genes in a wide range of endothelial lineage cells [Shichiri and Hirata, 2001]. Additional investigations by MacDonald et al. [2001], which demonstrated that internalized endostatin bound tropomysin-containing microfilaments of endothelial cells, provided a plausible mechanism for endostatin's inhibition of endothelial cell migration and invasion. Further, Lee et al. [2002] have shown a potential mechanism whereby endostatin suppresses cell invasion as their data show endostatin directly binds to the catalytic domain of matrix metalloproteinase-2 (MMP-2), thereby suppressing MMP-2's catalytic function. Cumulatively, these studies show endostatin's pleiotrophic effects are the consequence of diverse mechanisms that modulate numerous cellular pathways. Further clarification of these cellular mechanisms and identification of endostatin-responsive cell types could extend therapeutic applications of endostatin beyond inhibition of angiogenesis.

Because endostatin is recognized as a potent angiostatic agent, the vast majority of endostatin cell-based studies have employed endothelial cells. In contrast, this present study investigated whether endostatin modulates functional activities of KS tumor cells. We report, for the first time, that KS cells rapidly internalize endostatin and that endostatin initiates activation of the transcription activating factors nuclear factor-κB (NF-κB) and activating protein 1 (AP-1). We also show that internalized endostatin co-localizes to tropomysin microfilaments and acts to inhibit KS cell migration and invasion in response to the clinically relevant complete angiogenic cytokines bFGF and VEGF.

MATERIALS AND METHODS

Isolation and Characterization of AIDS-KS Cells

AIDS-KS cells were isolated from biopsy confirmed tumors of AIDS-KS as previously described [Mallery et al., 2000a]. These AIDS-KS strains have been shown to possess a normal XY karyotype and show aspects of a transformed phenotype including: high production of "KS" related cytokines such as IL-6, TNF-α, and bFGF, capacity to undergo multiple population doublings (>30) in reduced serum (0.5%) medium, and loss of anchorage dependence [Bailer et al., 1995]. Furthermore, relative to matched, nonlesional cells from the AIDS-KS donors, the KS spindle cells possess unique biochemical features including reduced cytoprotective enzyme function, increased responsiveness to pro-inflammatory cytokines, and reduced tolerance to chemotherapeutic agents that function by redox cycling [Mallery et al., 1999, 2000b]. The AIDS-KS cells were cultured at 37°C, 5% CO_2 in "complete" medium, which consisted of: M-199

(GIBCO, Grand Island, NY), supplemented with 15 mM HEPES, 0.23 mg/ml L-glutamine, 11 μg/ml sodium pyruvate, sodium heparin (Sigma, St. Louis, MO, 90 μg/ml), 10% heat inactivated fetal bovine serum (Hyclone, Logan, UT).

To reduce nonspecific integrin and matrix metalloproteinase expression due to the various cytokines and growth factors present in serum and provide a baseline from which to assess endostatin and/or cytokine responsiveness, cells were cultured in serum-free M-199 (base) medium for 72 h prior to conduction of either migration, invasion, and electromobility shift assays. While serum deprivation reduced mitotic indices and growth rates, cell viability remained comparable (>95%) to log growth conditions. KS cell strains (ks.1, ks.2, ks.3) isolated from three nodular phase intraoral KS tumors were used for these studies. These strains were selected due to their high histologic grade and aggressive clinical behavior, i.e., destruction of underlying alveolar bone and primary tumors of $\geq$1 cm.

Assessment of KS Cell Capacity to Internalize Biotinylated Endostatin

A total of 1×10^4 KS cells were plated on Lab-Tek chamber slides coated with 0.5 ml of poly-L-lysine (at a concentration of 0.1 mg/ml) and cultured in serum-free M-199 base medium for 24 h, followed by a 24 h incubation in base medium + 50 ng/ml bFGF. Endostatin (Calbiochem, La Jolla, CA) was biotin labeled using the Immunoprobe™ Biotinylation Kit (Sigma), with a final biotin:protein ratio of 2.2:1. The KS cells were then incubated with 10 μg/ml of biotinylated endostatin for specific periods (0, 5, 30, 90, 150 min) at 37°C, 5% CO_2. At the designated harvest points, slides were fixed (methanol and acetone washes), followed by the addition of Alex 488-conjugated avidin (Molecular Probes, Eugene, OR, final concentration 1 μg/ml in PBS) and ProLong Antifade mounting medium (Molecular Probes). Cell-associated endostatin was then determined by fluorescence microscopy.

Determination of Endostatin's Effects on Activation Status of NF-κB and AP-1 by Electromobility Shift Assays (EMSAs)

EMSAs were conducted to determine whether or not endostatin challenge activated KS cell membranes and initiated a signal transduction cascade. The experimental groups for these experiments were: (i) log growth, (ii) 72 h sera deprived (negative control), (iii) sera deprived, treated for 30 min with endostatin (10 μg/ml), (iv) sera deprived, treated for 30 min with TNF-α (100 U/ml, positive control). Nuclear and cytosolic extracts were prepared from trypsinized cells using a commercially available cell lysis buffer (NE-PER #78833, Pierce, Rockford, IL) which contained a protease inhibitor cocktail that was added to the lysis buffer just prior to use (Halt Protease inhibitor cocktail kit #78410, Pierce).

Every EMSA run included positive nuclear extracts [HeLa (AP-1 and NF-κB) from Promega, Madison, WI] as well as negative controls consisting of reagents without nuclear extracts. EMSAs were conducted using the LightShift Chemiluminescent EMSA kit (Pierce #20148). This method employs a nonisotopic method to detect DNA–protein interaction, and uses biotin end-labeled DNA that is detected using a streptavidin–horseradish peroxidase conjugate and a chemiluminescent substrate. EMSAs conducted using LightShift assays require biotin-labeled double-stranded DNA, with end-labeling of both complimentary oligonucleotides separately, followed by annealing at room temperature. The consensus oligonucleotide sequences (5′ to 3′) used were: ACT TGA GGG GAC TTT CCC AGG C (NF-κB, forward), GCC TGG GAA AGT CCC CTC AAC T (NF-κB, reverse); CGC TTG ATG AGT CAG CCG GAA (AP-1, forward), TTC CGG CTG ACT CAT CAA GCG (AP-1, reverse). Three assay controls, which consisted of biotin–EBNA control DNA only, biotin–EBNA control DNA and EBNA extract, and biotin–EBNA control DNA, EBNA extract, and a 200-fold molar excess of unlabeled EBNA DNA, were included in every EMSA conducted. A fourth KS strain (ks.4), which was also isolated from a patient with a nodular phase intraoral KS tumor, was included for the EMSA analyses.

Fluorescent Staining of KS Cells

KS cells (1×10^4) were plated on Lab-Tek chamber slides (Naperville, IL) coated with human plasma fibronectin (25 μg/ml), incubated overnight in proliferative growth medium (M-199 supplemented with 10% heat inactivated FBS), and then fixed in 10% neutral formalin, followed by a methanol wash in accordance with the methods of MacDonald et al., 2001. The

chamber slides were then incubated in PBS/1% FBS containing 20 μg/ml of Alexa 488 labeled rhEndostatin (Molecular Probes) for 1 h at room temperature, coverslips mounted using fluorescent mounting media, and cells photographed under Alexa excitation wavelength (absorption, 495 nm; emission, 519 nm). Co-localization studies were conducted as above with the exception that cells were incubated in PBS/1% FBS containing: 2.9 μg/μl mouse anti-tropomysin TM311 (Sigma) and 20 μg/ml of Alexa 488-labeled rhEndostatin followed by incubation with goat anti-mouse IgG (H + L). Studies were conducted with an isotypic control (2.9 μg/μl mouse IgG1, Chemicon, Temecula, CA) to confirm specificity of staining. The same fields were photographed under Alexa 488 (green, endostatin) and Alexa 594 (red, tropomysin) wavelengths. KS strains ks.1, ks.2, ks.3, and ks.4 were used for these studies.

Conduction of Cellular Migration and Invasion Assays

Both functional assays were conducted using the BD BioCoat FluoroBlok migration and invasion systems (Becton Dickinson, Bedford, MA). Because preliminary studies conducted in our laboratory showed that calcein loading was cell strain dependent, a standard curve was conducted using calcein-loaded cells from the same KS cell strain being assayed for each experiment. These assays are linear in the range of 2,000–50,000 calcein-loaded cells. Successfully migrated cells were quantitated using a fluorescence plate reader (excitation/emission 485/530 nm) with cell numbers determined using the concurrently run, same cell strain standard curve.

Trypsinized cells were loaded with the fluorescent dye Calcein-AM (Molecular Probes) [5 μg/ml, prepared in phosphate buffered saline (PBS)]. As preliminary studies showed that serum facilitated dye uptake, calcein loading was conducted for 2 h, 37°C, 5% CO_2 in optimal growth medium that contained 10% fetal bovine serum. Calcein-loaded cells were then resuspended in base medium and either treated (37°C, 5% CO_2) with endostatin (10 μg/ml, prepared in base medium, which remained present during the assay) or vehicle (base medium) for 30 min using gentle agitation to ensure uniform dispersion of endostatin. Cell viabilities (trypan blue exclusion) remained >95% following endostatin exposure. Previous studies conducted by our laboratory have shown an excellent agreement (viabilities comparing within 1%) between trypan blue exclusion and lactate dehydrogenase release assays [Mallery et al., 2000b]. Migration assays (5×10^4 cells/300 μl) were conducted at 37°C in 5% CO_2 for 4 h, using 50 ng/ml of either bFGF or VEGF as the chemoattractant. Invasion assays employed a 24 h incubation of 2.5×10^4 cells under similar conditions (37°C, 5% CO_2, with either 50 ng/ml bFGF or VEGF).

Statistical Analyses

The two-way Wilcoxon matched pairs test was used to evaluate endostatin's effects on KS cell migration and invasion. Differences >0.05 were considered to be statistically significant.

RESULTS

KS Cells Show Rapid Internalization and Degradation of Endostatin

KS cells showed a time dependent uptake and clearance of endostatin (Fig. 1). No staining was detected at time zero. Within 5 min, endostatin was membrane associated and had begun intracellular cytosolic distribution. By 30 min, the KS cells showed a punctate intracellular endostatin distribution, suggestive of mitochondrial uptake. Within 90 min, intranuclear deposition of endostatin was apparent. After 150 min, KS cells showed a marked reduction in endostatin staining, suggestive of endostatin clearance and/or metabolism. Notably, KS cell morphology was altered by endostatin uptake. In contrast to the "classic" spindle cell morphology, endostatin incorporation resulted in flatter cells that lacked cell extensions (Fig. 1). All three KS strains tested showed similar kinetics, intracellular distributions, and morphologic alterations following uptake of biotinylated endostatin.

Soluble Endostatin Induces Activation and Nuclear Translocation of Nuclear Factor κB (NF-κB) and Activating Protein 1 (AP-1) in a KS Strain Dependent Fashion

Following sera deprivation, there was a predicted decrease in activation status of both NF-κB and AP-1 in each KS strain (Fig. 2). All KS cell strains responded to the positive control (100 U/ml of TNFα) with activation and nuclear translocation of NF-κB (Table I). In addition, TNFα activated AP-1 in all of the KS strains

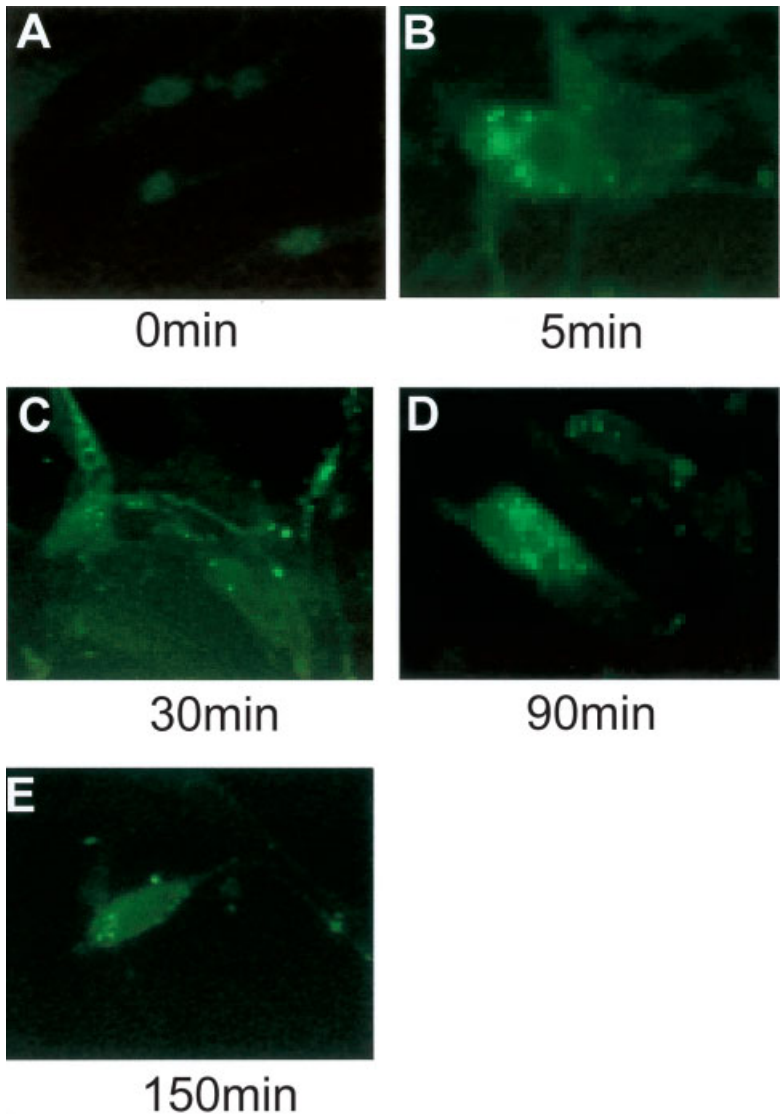

Fig. 1. Kaposi's sarcoma cells show rapid internalization and degradation of endostatin. A total of 1×10^4 KS cells were plated on Lab-Tek chamber slides coated with 0.5 ml of poly-L-lysine at a concentration of 0.1 mg/ml, and cultured in serum-free M-199 base medium for 24 h, followed by a 24 h incubation in base medium + 50 ng/ml bFGF. The KS cells were then incubated with 10 μg/ml of biotinylated endostatin for specific periods (0, 5, 30, 90, 150 min) at 37°C, 5% CO_2. At the designated harvest points, slides were fixed (methanol and acetone washes), followed by the addition of Alex 488-conjugated avidin and ProLong Antifade mounting medium. Cell-associated endostatin was then determined by fluorescence microscopy. Our results show a lack of staining at 0 min (**A**), and that by 5 min endostatin is both membrane associated and beginning intracellular cytosolic distribution (**B**). By 30 min (**C**), KS cells show a punctate, intracellular distribution of endostatin, suggestive of mitochondrial uptake. By 90 min (**D**), punctate, intranuclear distribution of endostatin is apparent. At the 150-min time point (**E**), KS cells show a marked reduction in staining, indicating either degradation and/or clearing of endostatin. All photomicrographs are shown at 400 × image scale, ks.1 strain.

with the exception of ks.4, albeit at lower levels relative to NF-κB. Endostatin challenge resulted in activation and nuclear translocation of NF-κB in each KS strain except ks.2. While endostatin exposure elicited AP-1 activation in ks.1 and ks.3 cultures, strain ks.2 was again refractory to endostatin challenge. The ks.4 strain failed to activate AP-1 following challenge with either TNFα or endostatin.

Recombinant Human Endostatin and Tropomysin Co-Localize to KS Cell Microfilaments

Co-localization studies showed that KS cells localized Alexa 488-labeled endostatin (green)

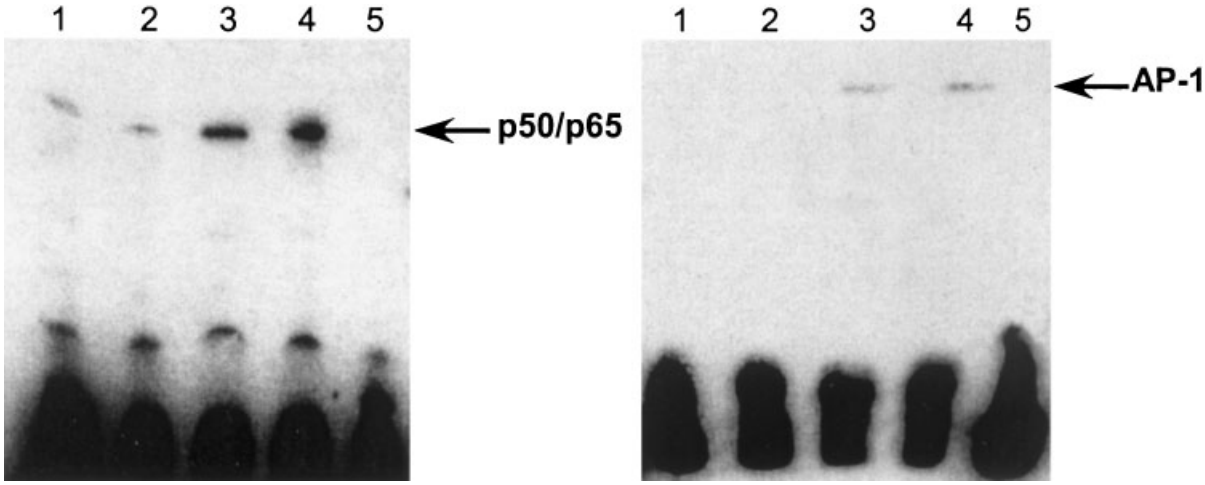

Fig. 2. Soluble endostatin causes nuclear translocation of nuclear factor κB (NF-κB) and activating protein 1 (AP-1) in KS cells. Cells were cultured for 72 h in serum free M-199 base medium to provide a baseline from which to assess endostatin's effects on transcription activating factors. The experimental groups for the nuclear extract preparations were as follows: (i) log growth, (ii) 72 h sera deprived (negative control), (iii) sera deprived, treated for 30 min with endostatin (10 μg/ml), (iv) sera deprived, treated for 30 min with 100 U/ml TNFα (positive control) (ks.1 strain). Nuclear and cytosolic extracts were prepared from trypsinized cells using a commercially available cell lysis buffer (NE-PER #78833, Pierce) which contained a protease inhibitor cocktail that was added to the lysis buffer just prior to use (Halt Protease inhibitor cocktail kit #78410, Pierce). Three assay controls, which consisted of biotin–EBNA control DNA only, biotin–EBNA control DNA and EBNA extract, and biotin-EBNA control DNA, EBNA extract, and a 200-fold molar excess of unlabeled EBNA DNA, were included in every EMSA conducted. EMSA lanes for both NF-κB and AP-1 were: 1, log growth; 2, sera deprivation; 3, endostatin treatment; 4, TNFα challenge; 5, no extract. Challenge with TNFα resulted in nuclear translocation of both NF-κB and AP-1. Endostatin challenge resulted in comparable levels of NF-κB and AP-1 activation and nuclear translocation.

within cytosolic microfilaments and within the nucleus (Fig. 3). Evaluation of these same fields under Alexa 594 wavelength (red), showed tropomysin staining of the same cytosolic microfilaments that had stained positively with the Alexa 488 (green) wavelength. Complete absence of staining was noted in the isotypic control slides (data not shown). Co-localization was confirmed by photography under both Alexa 488 and 594 wavelengths. Similar to the biotinylated endostatin internalization studies, all three KS cell strains evaluated showed co-localization of endostatin to tropomysin microfilaments.

Data summaries for the electromobility shift, endostatin internalization, and endostatin co-localization assays are presented in Table I.

Soluble Endostatin Significantly Inhibits Migration and Invasion of KS to bFGF and VEGF

Our results showed that endostatin significantly inhibited KS cellular migration and invasion in response to the KS relevant, complete angiogenic growth factors, bFGF and VEGF (Table IIA,B). Our studies also showed that bFGF elicited greater KS cell functional responses relative to VEGF for both the migration and invasion assays. Stain dependent

TABLE I. Data Summaries for the Electromobility Shift, Endostatin Internalization, and Endostatin Co-Localization Assays

Cell strain	EMSA NF-κB TNFα	EMSA NF-κB endostatin	EMSA AP-1 TNFα	EMSA AP-1 endostatin	Endostatin internalization	Endostatin tropomysin co-localization
ks.1	Nuclear translocation	Nuclear translocation	Nuclear translocation	Nuclear translocation	Yes (strong)	Yes
ks.2	Nuclear translocation	No response	Nuclear translocation	No response	Yes (moderate)	Yes
ks.3	Nuclear translocation	Nuclear translocation	Nuclear translocation	Nuclear translocation	Yes (moderate)	Yes
ks.4	Nuclear translocation	Nuclear translocation	No response	No response	Not conducted	Not conducted

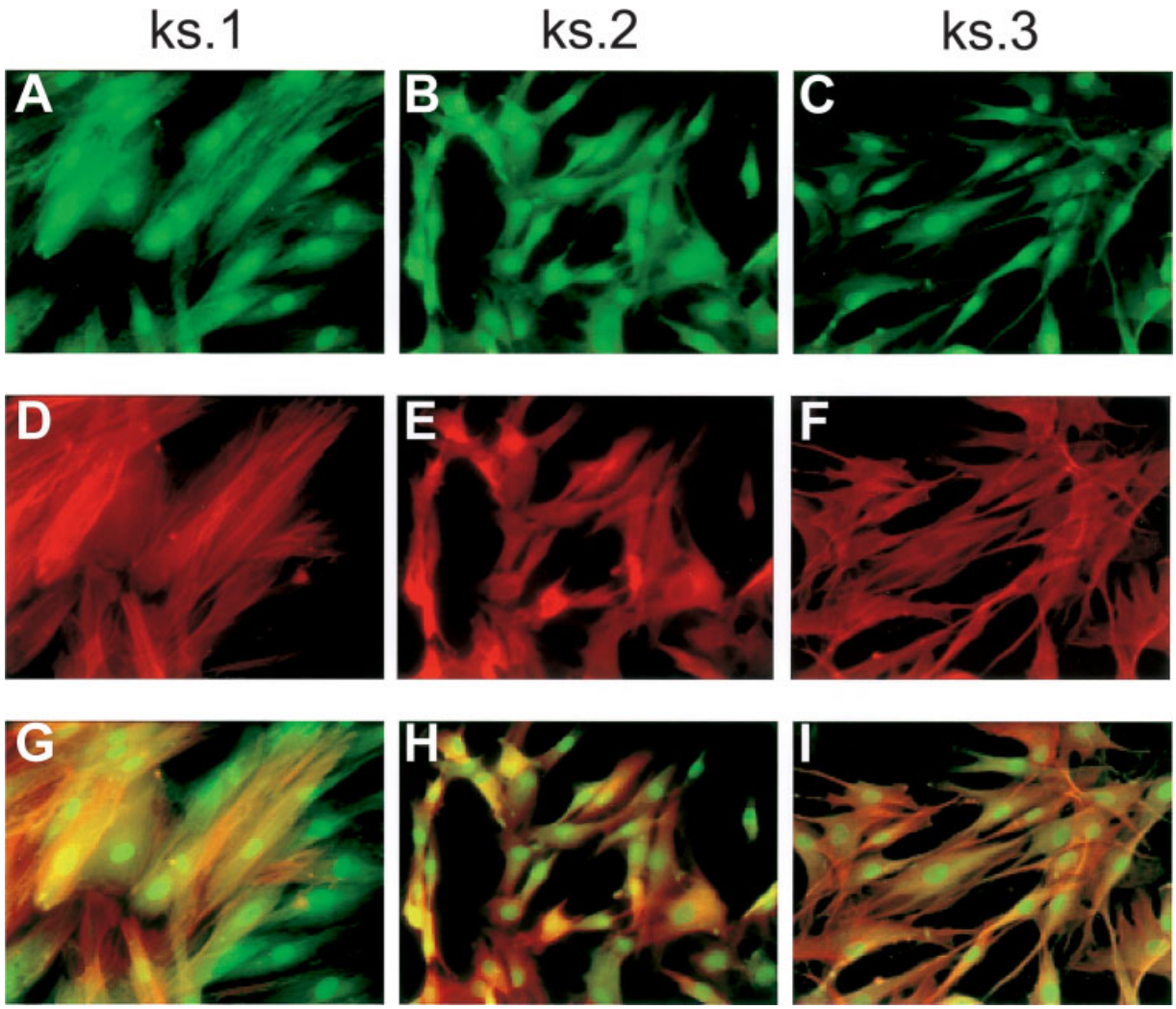

Fig. 3. Recombinant human endostatin binding and tropomysin co-localize to the microfilaments of KS cells. A total of 1×10^4 KS cells were plated on Lab-Tek chamber slides coated with human plasma fibronectin (25 μg/ml), incubated overnight in proliferative growth medium (M-199 supplemented with 10% heat inactivated FBS), and then fixed in 10% neutral formalin, followed by a methanol wash. The chamber slides were then incubated in PBS/1% FBS containing 20 μg/ml of Alexa 488 labeled rhEndostatin (Molecular Probes) for 1 h at room temperature, coverslips mounted using fluorescent mounting media, and cells photographed under Alexa excitation wavelength (absorption, 495 nm; emission, 519 nm). Co-localization studies were conducted as above with the exception that cells were incubated in PBS/1% FBS containing: 2.9 μg/μl mouse anti-tropomysin TM311 (Sigma) and 20 μg/ml of Alexa 488-labeled rhEndostatin followed by incubation with goat anti-mouse IgG (H&L). Studies were conducted with an isotypic control (2.9 μg/μl mouse IgG1, Chemicon) to confirm specificity of staining. The same fields were photographed under Alexa 488 (green, endostatin) and Alexa 594 (red, tropomysin) wavelengths. KS cells from two different donors were used for these studies (donor ks.1 shown in Fig. 2A,C,E; donor ks.2 shown in Fig. 2B,D,F). All photomicrographs are shown at a 400 × image scale. KS cells (**A**, **B**, **C**) localize Alexa 488-labeled endostatin (green) within cytosolic microfilaments and within the nucleus. The same fields (**D**, **E**, **F**), photographed under Alexa 594 wavelength (red), show tropomysin staining of the cytosolic microfilaments. Depicted in **G**, **H**, and **I** are the same fields photographed under both Alexa 488 and Alexa 594 wavelengths. Complete absence of staining was noted in the isotypic control slides (data not shown) [strain ks.1(A, D, G), ks.2 (B, E, H), ks.3 (C, F, I)].

differences were apparent as the ks.1 strain demonstrated the lowest migration and invasion responses to either VEGF or bFGF, regardless of experimental conditions (Table IIA,B, Fig. 4).

Migration assays showed that 10 μg/ml of soluble endostatin inhibited KS cellular migration to VEGF ($P < 0.001$) and bFGF ($P < 0.001$) (Table IIA and Fig. 4A). Inclusion of endostatin significantly decreased KS cell migration by

TABLE II. Individual KS Cell Strain Results of Functional Migration and Invasion Assays

Cell strain	Control + VEGF	Endostatin + VEGF	Percent change (%)	Control + bFGF	Endostatin + bFGF	Percent change (%)
Migration results (A)						
ks.1 n = 5 VEGF n = 5 bFGF	10,678 + 7,468	6,122 + 2,146	−43	19,452 + 3,100	10,420 + 2,121	−46
ks.2 n = 4 VEGF n = 5 bFGF	19,261 + 4,430	16,310 + 1,792	−15	36,351 + 3,209	28,850 + 3,227	−20
ks.3 n = 4 VEGF n = 6 bFGF	29,809 + 2,325	20,775 + 2,525	−30	47,698 + 2,001	38,962 + 3,861	−18
Invasion results (B)						
ks.1 n = 4 VEGF n = 3 bFGF	9,711 + 1,475	7,888 + 1,957	−19	8,777 + 1,567	7,607 + 2,179	−13
ks.2 n = 4 VEGF n = 3 bFGF	15,557 + 2,930	9,951 + 3,648	−36	18,155 + 1,820	9,988 + 3,651	−45
ks.3 n = 3 VEGF n = 4 bFGF	14,182 + 1,695	6,467 + 1,899	−54	19,378 + 5,238	10,378 + 5,238	−46

Functional assays were conducted using BD BioCoat FluoroBlok migration and invasion systems as described in Materials and Methods. Data are expressed as means of cell numbers + SEM. Endostatin inhibited migration in response to VEGF ($P < 0.001$), and bFGF ($P < 0.001$), as well as invasion in response to VEGF ($P < 0.001$) and bFGF ($P < 0.01$).

28% (VEGF, $P < 0.001$) and 24% (bFGF, $P < 0.001$). The individual cell line migration data are shown in Table IIA.

The uniform layer of Matrigel Basement Membrane Matrix contained in the BD BioCoat™ FluoroBlok™ Invasion System provides cells with conditions that simulate an intact basement membrane that provides a true barrier to noninvasive cells. Therefore, this assay permits a quantifiable and reproducible in vitro assessment of cellular invasive properties. Soluble endostatin significantly inhibited KS cellular invasion to response to VEGF ($P < 0.001$) and in response to bFGF ($P < 0.01$), Figure 4B. Inclusion of endostatin decreased KS invasion by 35% (VEGF) and 40% (bFGF). The individual cell line invasion data are shown in Table IIB.

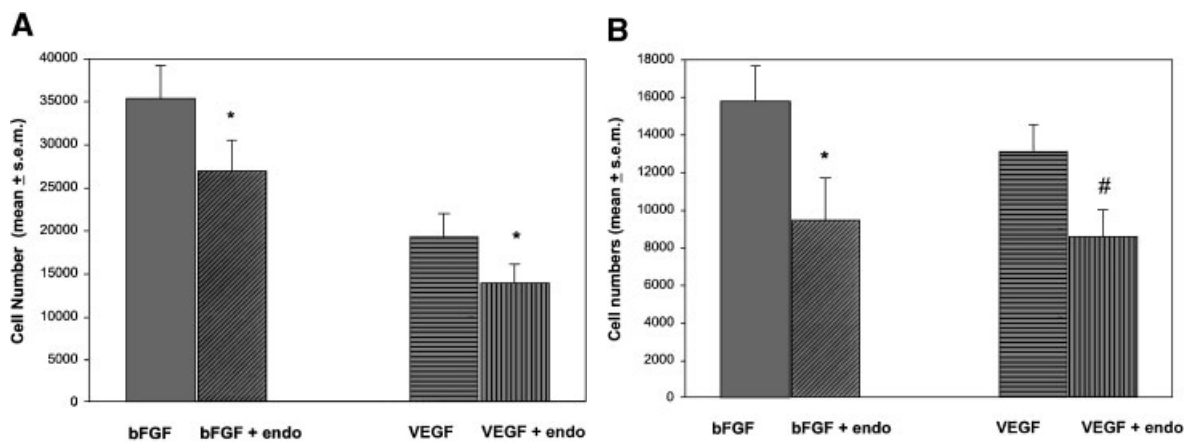

Fig. 4. Endostatin significantly inhibits migration and invasion of Kaposi's sarcoma (KS) cells to both basic fibroblast growth factor (bFGF) and vascular endothelial growth factor (VEGF). Both the migration and invasion assays were conducted using the BD BioCoat systems. The BD Invasion System simulates an intact basement membrane, thereby providing a true barrier to noninvasive cells. Migration assays (5.0×10^4 cells/300 µl, **A**) were conducted at 37°C, 5% CO_2 for 4 h, using 50 ng/ml of either bFGF or VEGF as the chemoattractant. Invasion assays (2.5×10^4 cells/300 µl, **B**) were conducted under similar conditions for 24 h. Successfully migrated or invasive cells were quantitated using a fluorescence plate reader with cells numbers determined using the concurrently run, same cell strain standard curve (n = 13 VEGF migration, n = 16 bFGF migration, n = 11 VEGF invasion, n = 10 bFGF invasion, n = 10 bFGF invasion, * = $P < 0.001$, # = $P < 0.01$).

DISCUSSION

Nodular KS lesions, which are the most advanced tumor stage, are histologically sarcomas that behave in a clinically aggressive fashion [McGarvey et al., 1998]. Our laboratory has previously shown that KS stains isolated from nodular KS tumors retain many features of a transformed phenotype such as sustained proliferation in serum-deficient medium and high autologous production of KS associated growth factors [Bailer et al., 1995]. This present study used cells isolated from nodular KS tumors in order to assess endostatin's effects on KS strains that possess the most malignant phenotype.

Results of our biotinylated endostatin studies showed that vital KS cells rapidly internalized endostatin. There are two potential mechanisms, which are not mutually exclusive, which could account for these findings. First, as endostatin is a naturally occurring substance, it is predictable that cells associated with angiogenesis such as endothelial lineage cells, possess an endostatin specific receptor. Alternatively, endostatin may be internalized via phagocytosis. This latter possibility is supported by previous studies from our laboratory that show KS cells are actively phagocytic [Mallery et al., 2000b]. The kinetic data show KS intracellular endostatin levels dramatically decreased within 150 min; implying either endostatin metabolism and/or export by KS cells. Our biotinylated endostatin intracellular distribution and kinetic data compare favorably with the work of Dixelius et al. [2000], who evaluated endostatin internalization and clearance in murine brain endothelial cells.

NF-κB and AP-1 are both pleiotrophic transcription factors that are activated by numerous stimuli including changes in the cell redox potential and cell membrane activation [Stall et al., 1994; Janssen-Heininger et al., 2000]. Activation of the integrin-linked kinase (ILK) is also known to activate AP-1 [Yoganathan et al., 2000]. Relevant to the ILK pathway, our laboratory has confirmed expression of the ILK associated integrin subunits β1 and β3 in each KS cell strain used in this study (data not shown). Our EMSA data show endostatin activated NF-κB and AP-1 in a cell-strain dependent fashion. These findings imply endostatin–integrin and/or endostatin–membrane interactions activate signaling pathways such as the ILK and suggest that integrin subunit expression may be a critical factor in determining whether or not endostatin challenge initiates signal transduction. Our results, which show endostatin initiates transcription factor activation, may initially appear contradictory to the findings of Shichiri and Hirata [2001], who showed that endostatin exposure down-regulated growth-associated genes in endothelial cells. Notably, both our biotinylated and fluorescent labeling studies showed endostatin intranuclear localization. We speculate that intranuclear endostatin impedes transcription factor binding to its DNA cognate binding site, potentially via steric hindrance, thereby reducing transcription factor mediated gene expression.

The co-localization of internalized endostatin to tropomysin microfilaments that was observed in all three KS cell strains examined suggests that this may be the underlying mechanism for the inhibitory activity of endostatin on KS cell migration and invasion. Our fluorescent staining results agree favorably with the findings of MacDonald et al., 2001, who identified hTM3 as an endostatin-binding tropomysin epitope in a variety of large and small vessel derived endothelial cells. Since tropomysin fulfills crucial role in actin stabilization and reorganization of the cytoskeleton [Lin et al., 1997], it is not surprising that tropomysin-binding agents could suppress cell motility.

Although cell migration and invasion frequently occur concurrently or sequentially, these cellular functions are related but distinct processes. While migration entails integrin upregulation and specific interactions with extracellular substrates, invasion also requires upregulation and activation of proteolytic enzymes [Murphy and Bavrilovic, 1999; Stamenkovic, 2000]. Our data show that short-term endostatin exposure inhibited both of these functions in KS cells isolated from three different donors. Our results also show that relative to VEGF, bFGF initiated higher levels of migration and invasion in all KS strains, suggesting increased bFGF receptor expression and/or bFGF is superior as a KS cell chemoattractant. Differences were also apparent among the KS strains with regard to baseline mobility as well as endostatin responsiveness. These data likely reflect a variety of KS interstrain cellular differences including numbers of VEGF and bFGF receptors, cellular capacity to increase expression of pro-migratory integrins

such as $\alpha_v\beta_6$, and ability to activate basement membrane degrading proteolytic enzymes such as MMP-2 and MMP-9. Because modulation of the patterns of integrin expression alters the ability of cells to interact with the extracellular matrix [Parise et al., 2000], we surmise that endostatin's abilities to interact with integrins acts in conjunction with endostatin–tropomysin interactions to inhibit KS cell migration and invasion.

Our functional assay data are in agreement with the findings of Rehn et al. [2001], which showed soluble endostatin served as an integrin antagonist for endothelial origin cells. In addition, the endostatin concentration [10 μg/ml (4.71×10^{-7} M)] used in our KS cell studies is comparable or lower than endostatin concentrations that have demonstrated efficacy during in vitro endothelial cell studies [Dhanabal et al., 1999; Dixelius et al., 2000; Rehn et al., 2001; Shichiri and Hirata, 2001]. This dose consistency implies that KS cells have similar thresholds of endostatin responsiveness as nontransformed endothelial cells.

There are several reasons why endostatin is an attractive agent for AIDS-related KS therapy. KS lesional cells both produce and respond to the complete angiogenic cytokines VEGF and bFGF. Therefore, the "proangiogenic phenotype" is inherent to KS tumor cells and also crucial for KS lesional progression. In addition, our data show endostatin directly inhibits KS cell migration and invasion. As a consequence of its combined angiostatic and antitumorigenic activities, endostatin could provide dual therapeutic benefits for KS.

Although human clinical trials with intravenously administered endostatin have not proven highly successful, subsequently conducted animal studies that used osmotic pumps that provided sustained endostatin drug levels demonstrated greater efficacies [Kisker et al., 2001]. These data suggest that intravenous delivery may not achieve and sustain optimal therapeutic endostatin concentrations, thereby reducing endostatin's efficacy. Notably, KS lesions often occur at visibly accessible mucocutaneous sites, which are amenable to use of locally injectable, biodegradable, controlled-release drug delivery systems. Controlled-release delivery vehicles provide sustained dosing rates and high intralesional drug concentrations without systemic side effects. These properties convey a pharmacologic advantage by increasing the drug's therapeutic index relative to systemic delivery [Toguchi, 1995]. While it is established that sustained controlled-release of bioactive proteins and peptides is technically challenging, our laboratories have demonstrated the ability to stabilize and provide sustained controlled-release of bioactive proteins from biodegradable polylactide-co-glycolide (PLGA) delivery vehicles [Zhu et al., 2000].

Currently advocated therapies for AIDS-associated malignancies therapies are designed to limit disease progression without exacerbating the underlying immune suppression [Shah et al., 2002]. We propose that locally injectable PLGA controlled-release endostatin delivery systems, which would combine endostatin's angiostatic and antitumorigenic effects without inducing deleterious systemic effects, could provide an effective and novel treatment for mucocutaneous AIDS-KS.

REFERENCES

Bailer RT, Lazo A, Ng-Bautista CL, Hout BL, Ness GM, Hegtvedt AK, Blakeslee JR, Stephens RE, Mallery SR. 1995. Correlation between AIDS-related Kaposi sarcoma histologic grade and in vitro behavior: Reduced exogenous growth factor requirements for isolates from high grade lesions. Lymphology 28:473–483.

Dhanabal M, Ramchandran R, Waterman MJF, Knebelmann B, Segal M, Sukhatme VP. 1999. Endostatin induces endothelial cell apoptosis. J Biol Chem 274: 11721–11726.

Dixelius J, Larsson H, Saski T, Holmqvist K, Lu L. 2000. Endostatin-induced tyrosine kinase signaling through the Shb adaptor protein regulates endothelial cell apoptosis. Blood 95:3403–3411.

Folkman J. 1995. Clinical application of research on angiogenesis. New Engl J Med 333:1757–1763.

Folkman J, Shing Y. 1992. Angiogenesis J Biol Chem 267: 10931–10934.

Gasparini G. 1999. The rationale and future potential of angiogenesis inhibitors in neoplasia. Drugs 58:17–38.

Jacobson LP, Arnemian HK. 1995. An integrated approach to the epidemiology of Kaposi's sarcoma. Curr Opin Oncol 7:450–455.

Janssen-Heininger YMW, Poynter ME, Baeuerle PA. 2000. Recent advances towards understanding redox mechanisms in the activation of nuclear factor κB. Free Radic Biol Med 28:1317–1327.

Kisker O, Becker CM, Prox D, Fannon M, D'Amato R, Flynn E, Fogler WE, Sim BKL, Allred EN, Pirie-Shepherd SR, Folkman J. 2001. Continuous administration of endostatin by intraperitoneally implanted osmotic pump improve the efficacy and potency of therapy in a mouse xenograft tumor model. Cancer Res 61:7669–7674.

Lee S-J, Jang J-W, Kim Y-M, Lee HI, Jeon JY, Kwon Y-G, Lee S-T. 2002. Endostatin binds to the catalytic domain

of matrix metalloproteinase-2. FEBS Letts 519:147–152.

Lin JJ, Warren KS, Wanboldt DD, Want T, Lin JL. 1997. Tropomysin isoforms in nonmuscle cells. Int Rev Cytol 170:1–38.

MacDonald NJ, Shivers WY, Narum DL, Plum SM, Wingard JN, Fuhrmann SR, Liang H, Holland-Linn J, Chen DHT, Sim BKL. 2001. Endostatin binds tropomysin: A potential modulator of the antitumor activity of endostatin. J Biol Chem 276:25190–25196.

Mallery SR, Clark YM, Ness GM, Minahawi OM, Pei P, Hohl CM. 1999. Thiol redox modulation of doxorubicin mediated cytotoxicity in cultured AIDS-related Kaposi's sarcoma cells. J Cell Biochem 73:259–277.

Mallery SR, Pei P, Kang J, Zhu G, Ness GM, Schwendeman SP. 2000a. Sustained angiogenesis enables in vivo transplantation of mucocutaneous derived AIDS-related Kaposi's sarcoma cells in murine hosts. Carcinogenesis 21:1647–1653.

Mallery SR, Pei P, Kang J, Ness GM, Ortiz R, Touhalisky JE, Schwendeman SP. 2000b. Controlled release of doxorubicin from poly(lactide-co-glycolide) microspheres significantly enhances cytotoxicity against cultured AIDS-related Kaposi's sarcoma cells. Anticancer Res 20: 2817–2826.

Masood R, Cai J, Zheng T, Smith D, Naidu Y, Gill PS. 1997. Vascular endothelial growth factor/vascular permeability factor is an autocrine growth factor for AIDS-Kaposi sarcoma. Proc Natl Acad Sci USA 94:979–984.

McGarvey ME, Tulpule A, Cai J, Zheng T, Masood R, Espina B, Arora N, Smith DL, Gill PS. 1998. Emerging treatments for epidemic (AIDS-related) Kaposi's sarcoma. Curr Opin Oncol 10:413–421.

Miles D. 1994. Pathogenesis of HIV-related Kaposi's sarcoma. Curr Opin Oncol 6:497–502.

Miles S, Rezai A, Salazar-Gonzalez J, Van der Meyden M, Stevens R, Logan D, Mitsuqasu R, Laza L, Hirano L, Kishimoto L, Martinez-Nazo O. 1990. AIDS Kaposi's sarcoma-derived cells produce and respond to IL-6. Proc Natl Acad Sci USA 87:4068–4071.

Murphy G, Bavrilovic J. 1999. Proteolysis and cell migration: Creating a path? Curr Opin Cell Biol 11:614–621.

O'Reilly MS, Boehm T, Shing Y, Fukai N, Vasios G, Lane WS, Flynn E, Birkhead JR, Olsen BR, Folkman J. 1997. Endostatin: An endogenous inhibitor of angiogenesis and tumor growth. Cell 88:277–285.

Parise LV, Lee JW, Juliano RL. 2000. New aspects of integrin signaling in cancer. Cancer Biol 10:407–414.

Rehn M, Veikkola T, Valdre-Kukk E, Nakamura H, Ilmonen M, Lombardo DR, Pihlajaniemi T, Alitalo K, Vuori K. 2001. Interaction of endostatin with integrins implicated in angiogenesis. Proc Natl Acad Sci USA 98: 1024–1029.

Rutger JL, Wieczorek R, Bintti F, Kaplan KL, Posnett DN, Friedman-Kein AE, Knowles DM. 1986. The expression of endothelial cell surface antigens by AIDS-associated Kaposi's sarcoma: Evidence for a vascular endothelial cell origin. Am J Pathol 122:493–499.

Samaniego F, Markhan PD, Gendelman R, Watanabe Y, Kao V, Kowalsek K, Sonnabend JA, Pintus A, Gallo RC, Ensoli B. 1998. Vascular endothelial growth factor and basic fibroblast growth factor present in Kaposi's sarcoma are induced by inflammatory cytokines and synergize to promote vascular permeability and KS lesion development. Am J Pathol 152:1433–1443.

Shah MH, Porcu P, Mallery SR, Caligiuri MA. 2002. Chapter 31: AIDS-associated malignancies. In: Giaccone G, Schilsky R, Sondel P, editors. Cancer chemotherapy and biological response modifiers, Elsevier Science B.V. p 633–664.

Shichiri M, Hirata Y. 2001. Antiangiogenesis signals by endostatin. FASEB 15:1044–1053.

Stall FJT, Anderson MT, Staal GEJ, Herzenberg LA, Gitler C, Herzenberg LA. 1994. Redox regulation signal transduction: Tyrosine phosphorylation and calcium influx. Proc Natl Acad Sci USA 91:3619–3622.

Stamenkovic I. 2000. Matrix metalloproteinases in tumor invasion and metastasis. Cancer Biol 10:415–4333.

Toguchi H. 1995. Biodegradable microspheres in drug delivery. Crit Rev Ther Drug Carr Sys 12:1–99.

Yoganathan TN, Costello P, Chen X, Jabali M, Yan J, Leung D, Zhang Z, Yee A, Dedhar S, Sanghera J. 2000. Integrin-linked kinase (ILK): A "hot" therapeutic target. Biochem Pharmacol 60:1115–1119.

Zhu G, Mallery SR, Schwendeman SP. 2000. Stabilization of proteins encapsulated in poly(lactide-co-glycolide). Nat Biotechnol 18:52–57.